Computational fluid dynamics simulation of natural gas hydrate sloughing and pipewall shedding temperature profile: implications for CO2 transportation in subsea pipeline.

UMUTEME, O.M., ISLAM, S.Z., HOSSAIN, M. and KARNIK, A.

2023

CRediT author statement

Computational Fluid Dynamics Simulation of Hydrates Sloughing and Pipewall Shedding by Hydrates in Subsea Gas Pipelines

Oghenethoja Monday Umuteme, Sheikh Zahidul Islam*, Mamdud Hossain and Aditya Karnik
School of Engineering, Robert Gordon University, Aberdeen, AB10 7GJ, UK
*Corresponding author. Email: s.z.islam1@rgu.ac.uk
Phone: +44(0)1224 262319
Fax: +44(0)1224 262444

Oghenethoja M. Umuteme: Conceptualization, Methodology, Software, Validation Data curation, Writing- Original draft preparation, Visualization, Investigation. ***Sheikh Zahidul Islam****:* Supervision, Conceptualization, Writing- Reviewing and Editing**. Mamdud Hossain:** Supervision, Writing- Reviewing and Editing. **Aditya Karnik:** Supervision, Writing- Reviewing and Editing.

Computational Fluid Dynamics Simulation of Natural Gas Hydrate Sloughing and Pipewall Shedding Temperature Profile: Implications for CO_2 Transportation in Subsea Pipeline

Oghenethoja Monday Umuteme, Sheikh Zahidul Islam*, Mamdud Hossain and Aditya Karnik
School of Engineering, Robert Gordon University, Aberdeen, AB10 7GJ, UK
*Corresponding author. Email: s.z.islam1@rgu.ac.uk
Phone: +44(0)1224 262319
Fax: +44(0)1224 262444

Abstract-

The continuous flow assurance in subsea gas pipelines heavily relies on the assessment of temperature profile during hydrate sloughing and pipewall shedding caused by hydrates, with similar implications for carbon dioxide (CO_2) transportation under hydrate-forming conditions. Hydrate sloughing is the peeling off of some hydrate deposits from the pipeline inner surface. Similarly, pipewall shedding by hydrates involves the direct interaction of hydrates with the pipeline inner surface, resulting in the detachment or removal of hydrate deposits from the pipewall. While sloughing occur within the deposit of hydrates, pipewall shedding is related to direct interaction of the gas phase with the thin layer of hydrates on the pipewall. In this study, a computational fluid dynamics (CFD) simulation approach is employed, using a validated CFD model from the literature for predicting hydrate deposition rates (Umuteme et al., 2022), by applying a subcooling temperature to the pipe wall at hydrates forming condition. We have deduced the presence of hydrates based on the stable temperature profile of natural gas hydrates along the pipeline model. The study shows that the simulated temperature contours align well with the reported hydrate deposition profile in gas pipelines (Di Lorenzo et al., 2018). The conversion of the consumption rate of natural gas to hydrates was achieved using the equation proposed in the literature (Umuteme et al., 2022). Two shear stress regimes have been identified for hydrate sloughing and pipewall shedding in this study, with the latter resulting in higher shear stress on the pipewall. Presently, there is a growing concern regarding the potential leakage of CO_2 in pipelines (Lu et al., 2020; Wang et al., 2022; Wareing et al., 2016), which may escalate due to pipewall corrosion caused by hydrates (Obanijesu, 2012). The findings in this research can provide further knowledge that can enhance the safe transportation of CO_2 in pipelines under stable hydrate forming conditions.

Hydrates Deposition Rates; CFD modelling; Hydrates Sloughing; Shear Stress; Pipewall shedding; Shear Strain

Highlights

- CFD modelling of hydrates sloughing and pipewall shedding is proposed.
- Pipewall shedding and sloughing are concurrent at higher gas flow velocity
- The sloughing angle decreases as the gas velocity increases
- Hydrates sloughing and pipewall shedding are driven by inertia force

Graphical abstract

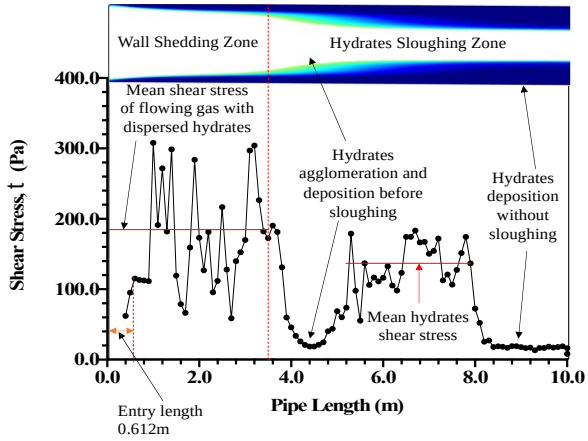

1. Introduction-

Hydrate sloughing or pipewall shedding is essential in the study of hydrate deposition, transportability and pipeline plugging by hydrates. Hydrate sloughing is the peeling off of some hydrate deposits from the pipeline inner surface (Aman et al., 2016; Liu et al., 2019). Similarly, pipewall shedding by hydrates, as defined in the current study, involves the direct interaction of hydrates with the pipeline inner surface, resulting in the detachment or removal of hydrate deposits from the pipewall. This study posits that sloughing within the hydrate deposits results in a thin layer of hydrate on the inner surface of the pipeline. However, pipewall shedding effectively removes all remaining hydrates from the pipewall. Evidence in the literature suggests the difficulty in modelling sloughing events because of the complicated nature of the deposition of hydrates in gas-dominant pipelines (Charlton et al., 2018b). Transient sloughing events are responsible for the fluctuating pressure drop during the operation of gas-dominant pipelines (Di Lorenzo et al., 2014b). The sloughing of hydrates creates a non-uniform internal diameter profile at the sections where it occurs leading to a drop in the pressure drop (Di Lorenzo et al., 2014a; Liu et al., 2019). Thus, the study of the sloughing and shedding of hydrates can provide insights into the implementation of hydraulic flow control measures in monitoring the plugging of pipelines by hydrates. Moreover, research in gas pipeline hydrates has continue to attract research interest among academic and industry researchers in the last decade as evident from literature search. Related studies in gas pipelines, include hydrates nucleation, agglomeration, deposition and plugging, which can be explained by both hydrate formation kinetics and hydraulic flow models. Kinetics models provide insights into the nucleation and agglomeration of hydrates, while hydraulic models explain deposition and plugging. Agglomeration is the accumulation of hydrates into a large mass. Turner et al. (2005) developed a hydrates kinetics model that has gained increased acceptance in the modelling of hydrate growth kinetics by researchers with results that compares favourably with experimental outcomes (Charlton et al., 2018a; Liu et al., 2019; May et al., 2018; Zerpa et al., 2013). Also, our CFD model implemented the kinetics model in the user-defined functions (UDFs) for both mass and energy sources in Ansys Fluent (Umuteme et al., 2022). The source codes were implemented to control the accumulation of gas in the computational domain by mimicking the volumetric consumption rate of gas during hydrates formation. The increase of gas density at the pipewall in our previous study also mimicked the concentration of gas in deposited hydrates reported in the literature (Sloan, 2011). Again, the suggested ratio of gas-induced sloughing shear stress on the hydrate layer to the water-induced shear stress at the pipe wall agrees with similar metrics reported in the literature (Aman et al., 2018). Previous studies on the agglomeration, deposition, and plugging of hydrates have led to the following propositions. Jassim et al. (2010) suggests that agglomeration leads to the growth of hydrates up to a critical size before they are deposited, and that the depositional distance is a function of pipe diameter and velocity of the primary gas phase. Implying that hydrates smaller than the critical size are transported with a drift velocity farther away from the source of formation (Jassim et al., 2010).

Again, previous studies suggests that the deposition of hydrates on the pipe wall leads to plugging and propositions that the deposition of hydrates: (i) increases with velocity at constant subcooling temperatures; and (ii) increases with as the subcooling temperatures increases if the gas velocity remains constant (Aman et al., 2016; Di Lorenzo et al., 2014b). Subcooling temperature is the difference between the gas temperature and the ambient temperature of the pipeline surrounding. The four stages of hydrates formation, agglomeration, deposition, and plugging can be observed from temperature and pressure curves in the literature (Liu et al., 2020; Umuteme et al., 2022). Thus, the pressure drop at constant flow rate increases during hydrate formation and agglomeration, reduces during deposition, and increases again during plugging (Liu et al., 2020; Umuteme et al., 2022). For the temperature range of 284 - 287 K and constant pipeline operating pressure of 8.8 MPa and gas velocity of 4 m/s, a drop in pressure was observed at the onset of deposition and a steady rise in pressure until the line is fully plugged. This trend is also corroborated in the literature (Liu et al., 2020). Hydrates shedding at the pipe wall and sloughing occurs alongside deposition and leads to the transport of hydrates downstream of the formation equilibrium temperature and pressure condition along the pipeline. The deposited hydrates are transported downstream and closely packed at locations of reduced pipe annulus or at the base of offshore pipeline riser. Therefore, sloughing and wall shedding are related to the hydraulic effects of hydrates transportability. Both concepts are important in the study of hydrates because of the consequential fluctuation of transient pressure spikes. In some cases, the pipe can rupture before the safe-trip valves are activated when the pressure spikes are beyond the maximum incidental pressure of the gas pipeline. Analytical models in the literature (Di Lorenzo et al., 2018; Liu et al., 2019; Wang et al., 2017), have been conservative in the prediction of the transient pressure drop and plugging flowtime during hydrates formation in gas pipelines. Therefore, these models were unable to accurately predict hydrates sloughing and wall shedding sites along the pipeline section prone to hydrates. A better understanding of how both concepts occur can provide further insights into the relationship between hydrates plugging flowtime and the overall hydrates-induced gas flow dynamics. This nature of knowledge can aid the understanding of transportability of hydrates and the planning of mechanical intervention pigging activities.

Three basic factors can be identified as responsible for the increase in hydrates formation and deposition in gas-dominated pipelines. In this study, a pipeline is gas-dominated when the volume fraction of water is less than 7% otherwise, the pipeline is considered water-dominated. The scenarios for hydrates formation and deposition are encountered during: (i) seasonal temperature changes influencing the subcooling temperature at the same gas flowrate; (ii) operational need to increase gas production into the pipeline because of the development of new wells and the increasing demand for gas at a constant subcooling temperature; and (iii) the need to reduce gas supply at a constant subcooling temperature.

Previous hydrates deposition and sloughing predictive model by Di Lorenzo et al. (2018) was based on a geometry of hydrates deposition and sloughing along the pipeline. Later, Liu et al. (2019) developed a model that produced a profile of hydrates thickness that increased gradually from the inlet to the end of the 40 m length pipeline used for the study. The deposited layer of hydrates was reduced by hydrates shedding event at 18.3 m downstream of the inlet. However, both studies did not discuss pipewall shedding by hydrates happening upstream of the location where hydrates sloughing/shedding event occurs. Again, the profile presented in the literature indicates that some layers of hydrates were left on the pipewall during sloughing, which will eventually be eroded by the multiphase flow (gas-water-dispersed hydrates) happening behind the location of the sloughing event. We suggest that “pipewall shedding by hydrates” is interaction between the deposited hydrates layer and the pipe wall; and occurs after sloughing events. Nicholas et al.(2008) suggests that sloughing induces flow induced vibration in a hydrate forming pipeline, and that this is time-dependent on the rate of hydrate growth and the volume fraction. This prior understanding is premised on the fact that before hydrates are deposited, the dispersed hydrate in the multiphase flow interacts with the pipe wall and this effect can be examined from the fluctuating nature of the shear stress induced on the pipewall

by the viscous fluid. As the layer of hydrates grows, hydrates sloughing happens within the hydrates layer without eroding the pipewall (Straume et al., 2018).

The purpose of this paper is to further enrich the literature on the knowledge of natural gas transmission by studying pipewall shedding, which is a new concept different from hydrate sloughing and wall shedding. It is assumed in this study that pipewall shedding by hydrates is caused by dispersed hydrates in the multiphase flow behind the location of hydrates sloughing events. By plotting the hydrates-induced shear stress profile along the pipeline, higher shear stress zones were identified as possible locations of erosion-induced internal corrosion. Previous studies reports a positive relationship between flowing shear stress and increasing internal corrosion rate in a gas pipeline (Obanijesu, 2009). In our previous work (Umuteme et al., 2022) simulated the conditions for hydrate formation and the resulting shear stress. However, the location of hydrates sloughing event along the pipeline is not clear from the extant literature (Wang et al., 2018). This study closes this gap by fulfilling the following objectives, which include: (i) providing the flowing pipewall shear stress profile during hydrates formation and deposition under different gas velocities, (ii) suggesting a relationship between the hydrate sloughing location and gas flowing velocity, and (iii) investigating the influence of inertia force on hydrate sloughing and pipewall shedding to enhance the knowledge of the influence of inertia force on the transportability of hydrates. Based on the temperature of stable methane hydrates below 292K, we have inferred the location of hydrates sloughing and pipewall shedding along the gas pipeline model.

Similar to natural gas, carbon dioxide (CO_2) also forms stable hydrates in the presence of water and the principle of formation is similar (Bataille et al., 2018; Lu et al., 2020). When subjected to comparable operating conditions as natural gas, the more pronounced temperature reduction experienced by CO_2 inside the pipeline results in the earlier formation of hydrates compared to pipelines transporting natural gas (Lu et al., 2020). Currently, there is an increasing concern about the possible leak or rupture of CO_2 in pipelines (Lu et al., 2020; Wang et al., 2022; Wareing et al., 2016), a concern that could be exacerbated by the corrosion of pipeline walls caused by hydrate (Obanijesu, 2012). As a result, there is a heightened demand for enhanced diligence in the design of pipelines for transporting CO_2 (Barrie et al., 2005; Gough et al., 2014). Hence, understanding the formation and behaviour of CO_2 hydrates is important in carbon capture, utilization, and storage (CCUS) and CO_2 transport, as hydrate formation can impact the efficiency and safety of these processes. While the primary emphasis of this paper is the formation of hydrates in natural gas transportation pipelines, the findings of this study can offer valuable insights into the potential occurrence of sloughing and pipewall shedding in the event of the formation of carbon dioxide hydrates in pipelines. Therefore, the findings of this study can provide valuable insights for CO_2 transportation through pipelines. The remaining sections of this paper will discuss the methodology adopted, describe the CFD model, present approach to data analysis, define the input variables and boundary conditions, present the results and discussion, narrow the study to sloughing and pipewall shedding, and present the conclusion of major findings.

2. Methodology-

A eulerian-eulerian multiphase hydrate deposition rate CFD model that we developed and validated with empirical results in our previous paper discussed earlier (Umuteme et al., 2022), was used for the simulations in this study. The results were recorded at the subcooling pipewall temperature range of 2-8 K and velocity range of 2-8 m/s. Fig. 1 present the stages of the methodology adopted. The following main assumptions have been made:

- the primary and secondary phase inlet boundary conditions include a temperature of 292K and a pressure of 8.8MPa, respectively.

- pipewall shedding by hydrates is dependent on the magnitude of the shear stress on the pipewall and the strain rate of the deposited hydrates
- hydrates sloughing depends on the shear stress of the gas on the deposited hydrates and the resisting shear strength of the hydrate phase.
- pipewall shedding is possible when the shear stress of the multiphase is equal or greater than the shear stress of the water phase on the wall.
- hydrates sloughing occurs when the shear stress of the multiphase is greater than the shear strength of the deposited hydrates.
- the profile of deposited hydrates was inferred from the temperature contour of the gas phase; hence the study did not represent hydrate deposits along the pipeline as a discreet solid phase. In the subsequent sections of this paper, the formation and deposition of hydrates are inferred based on the temperature profile of the gas phase (<292K) at the pipeline inlet pressure of 8.8MPa for all simulations.
- The conversion of the consumption rate of natural gas to hydrates was achieved using Eq. (10) as proposed in the literature (Umuteme et al., 2022).

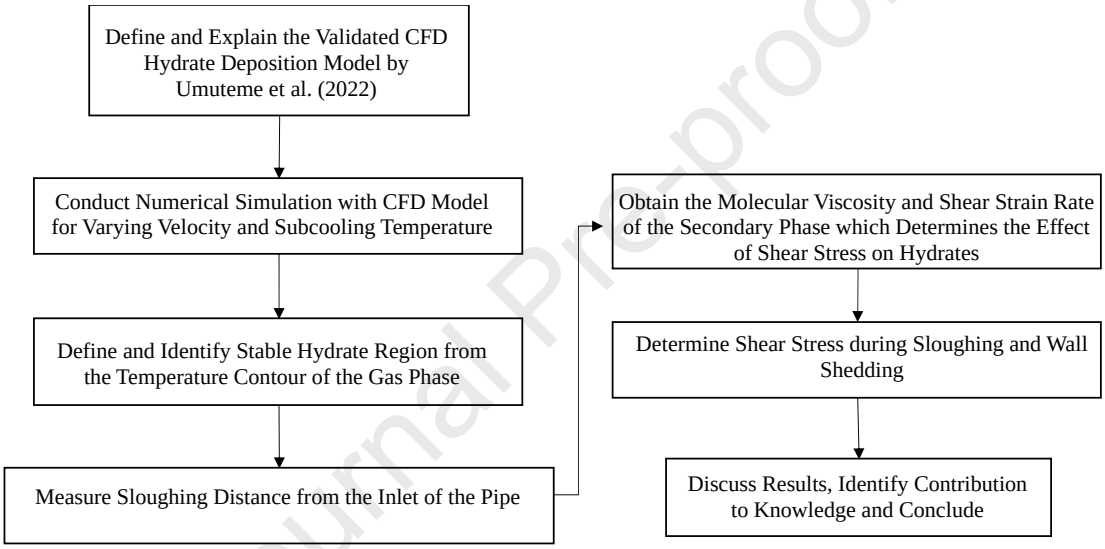

Fig. 1. A schematic representation of the adopted methodology

2.1 CFD Model Description

The model was developed in the literature (Umuteme et al., 2022), to mimic the deposition of hydrates on the internal pipewall by simulating the necessary boundary conditions of formation. Two UDF codes were employed in Ansys Fluent – one for the mass source and the other for the energy source. The mass source UDF code in C++ was from the mathematical relation of the kinetics model suggested in Turner et al. (2005) for gas consumption rate. The UDF code includes a conditional statement that checks whether the conditions satisfy the equation for hydrate equilibrium pressure at the operating temperature in the literature (Sloan and Koh, 2007). If the conditions are met, the code injects additional mass of methane gas to the computational domain. The energy source is the product of the gas injection rate and the hydrate heat of formation (Meindinyo et al., 2015). This energy source UDF also included the conditional statement as in the mass source UDF. The key role of the UDF codes is to add source terms into the continuity and energy conservation equations so that a controlled amount of gas is injected at the hydrate forming temperature and pressure conditions into the computational domain for every simulation time step. For each case, the calculation was performed over a duration of 4.0 seconds using a fixed time advancement approach, consisting of 40 time steps with a time step size of 0.1 seconds. The amount of gas injected is related to the consumption rate of gas during hydrate formation, and reduces during hydrates deposition (Aman et al., 2016; Odutola et al., 2017). The temperature of the gas reduces towards the

pipewall because of the sustained subcooling temperature at the pipewall, thus increasing the density of the gas (Umuteme et al., 2022). This condition influences the profile of the flowing shear stress at the pipewall. Although the pipewall was frictionless at the onset of hydrate formation, the pipewall shedding effect creates a wall friction which is resulting in the shear stress profile. The computational domain is a 10 m length by 0.0204 m diameter smooth pipe section. The numerical scheme was achieved with a 900000-cell 3D mesh which was adopted based on its lower transient pressure drop when compared with smaller and larger mesh sizes as presented (Fig. 2). The details of the approach for the mesh size selection is provided in our previous work (Umuteme et al., 2022).

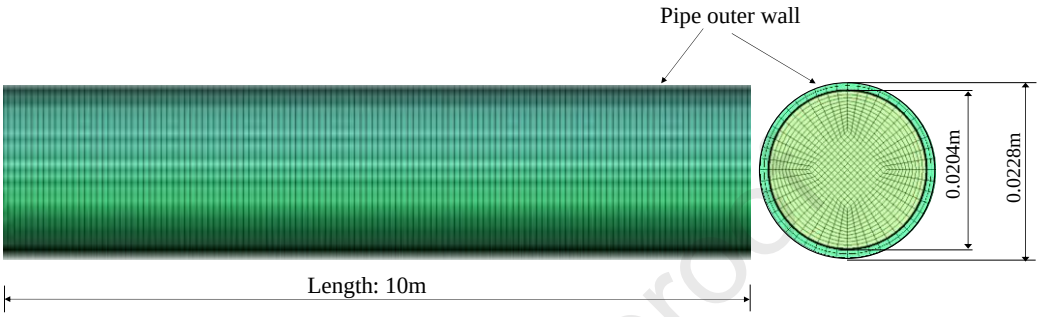

Fig. 2. 3D computational domain with meshed cells (not to scale)

The simulated multiphase flow includes methane gas as the primary phase and water as the secondary phase. In multiphase flow, the primary phase is the dominant continuous fluid that occupies the larger volume fraction of the flow, while the secondary phase is the dispersed phase in smaller fraction within the primary phase. Empirical results suggests that the solubility of methane in water increases at lower temperature and higher pressure (Lekvam and Bishnoi, 1997). Under the simulated hydrate forming pressure (8.8MPa) and temperature (<292K), the methane gradually dissolves in the water forming a solution enriched with methane. With increase in the dissolution of methane in water as the temperature drops further, the methane-rich solution will become supersaturated with methane, leading to the formation of hydrates. Since flow agitation increases hydrates formation (Carroll, 2014), we varied the velocity of the flow to investigate the influence of velocity on the temperature profile of the gas phase.

The conservative and turbulence equations implemented in the CFD model are presented as follows.

Continuity

$$\frac{\partial}{\partial t}\left(\alpha_q \rho_q\right) + \nabla.\left(\alpha_q \rho_q \vec{\vartheta}_q\right) = S_q \tag{1}$$

where for the primary (methane gas) and secondary phase (water) in the control volume, α_q is volume fraction; $\vec{\vartheta}_q$ is velocity (m/s); ρ_q is density (kg/m^3); and S_q is the source term implemented in a UDF code to control the rate of gas injection into the computational domain, as discussed earlier. Methane gas was simulated as natural gas, because natural gas is predominantly methane gas (Di Lorenzo et al., 2014a).

Momentum

$$\frac{\partial}{\partial t}(\overline{\alpha_c}\rho_c \tilde{u}_c) + \nabla.(\overline{\alpha_c}\rho_c \tilde{u}_c \otimes \tilde{u}_c) = -\overline{\alpha_c}\nabla\tilde{\rho} + \nabla.\overline{\alpha_q}\rho_q\left(\frac{2}{3}k - 2\frac{\mu_{t_q}}{\rho_q}.\nabla.\tilde{u}_c\right) \tag{2}$$

Eq. (*2*) is the Reynolds-Averaged Naiver-Stokes (RANS) momentum equation, where the carrier (gas) and q[th] phase are represented with the subscripts "c" and "q", respectively. The q[th] phase turbulent viscosity is, μ_{t_q}, which links the momentum equation to the $k-\varepsilon$ two-equation turbulence model (Eqs. (4) and (5)).

Energy

$$\frac{\partial}{\partial t}(\alpha_q \rho_q h_q) + \nabla.(\alpha_q \rho_q \vec{\vartheta}_q h_q) = -\alpha_q \frac{\partial \mathrm{p}_q}{\partial \mathrm{t}} + \bar{\bar{\tau}}_q : \nabla \vec{\vartheta}_q - \nabla.\vec{q}_q + S_q \quad (3)$$

where, h_q is specific enthalpy per phase; h_{pq} is interphase enthalpy; S_q is energy source due to the formation of hydrate, as discussed earlier; $\vec{q}_q$ is heat flux per phase; and $\frac{\partial \mathrm{p}_q}{\partial \mathrm{t}}$ is the transient pressure drop (Pa/s). The transient pressure drop is dependent on the dynamics of the viscous flow in the fluid domain during hydrates formation. The resulting shear stress is related to the resistance to fluid flow increase in gas density towards the pipewall during hydrates formation.

Turbulence models:

Multiphase CFD simulations incorporates turbulence models (Fox, 2014), to create the required turbulence that can promote interfacial area interaction between the primary and the secondary phase. The realizable $k-\varepsilon$ two-equation turbulence model in Eq.(4) and (5), have been implemented because it enhances near-wall viscous modelling (Wang et al., 2018). Near-wall viscous modelling is a term used in computational fluid dynamics (CFD) simulations to describe the techniques and methods employed to accurately represent the flow characteristics and boundary layer effects near solid surfaces such as inner pipeline surfaces as in this study. This modelling approach specifically targets the vicinity of walls where the fluid flow experiences significant influence from viscous effects.

Kinetic Equation:

$$\frac{\partial}{\partial t}(\alpha_q \rho_q k_q) + \nabla.(\alpha_q \rho_q \vec{\vartheta}_q k_q) = \nabla.\left(\alpha_q \left(\mu_q + \frac{\mu_{tq}}{\sigma_{\mathrm{kq}}}\right)\nabla k_q\right) + \alpha_q G_{kq} - \alpha_q \rho_q \epsilon_q + \alpha_q \rho_q \Pi_{k_q} \quad (4)$$

Dissipation Equation:

$$\frac{\partial}{\partial t}(\alpha_q \rho_q \varepsilon_q) + \nabla.(\alpha_q \rho_q \vec{\vartheta}_q \varepsilon_q) = \nabla.\left(\alpha_q \left(\mu_q + \frac{\mu_{tq}}{\sigma_{\varepsilon q}}\right)\nabla \varepsilon_q\right) + \alpha_q \frac{\varepsilon_q}{k_q}(C_{1\varepsilon} G_{kq} - C_{2\varepsilon} \rho_q \varepsilon_q) + \alpha_q \rho_q \Pi_{\varepsilon_q} \quad (5)$$

Furthermore, the closure parameters Π_{k_q} and Π_{ε_q}, represent the source terms that account for turbulence interactions between the entrained water phase and the primary gas phase, and have been defined for each phase as described in Simonin and Viollet (1990) and modified in Fluent Theory (2017). Six equations were solved including mass, momentum, energy, turbulence (kinetic and dissipation), volume fraction of each phase, and the interfacial area concentration for the dispersed phase modelling. The computation for each case lasted for 4.0 seconds with fixed-time advancement, and a time step size of 0.1 seconds. Simulations were stopped when the pressure drop increased excessively and the system experienced a back flow of gas mass flowrate. The average gas mass flowrate was monitored as a direct representation of the consumed gas for hydrates formation. The deposition of hydrates was estimated from the

pressure drop section that corresponds with the pressure categorisation in Liu et al. (2020). At this point, the transient temperature commenced an upward gradual rising profile. The results of the our hydrates deposition CFD model was validated with experimental data in the literature (Aman et al., 2016; Di Lorenzo et al., 2014a), and the transient pressure and temperature curves predicted by the CFD model also produced the stages of hydrates formation, agglomeration, deposition and plugging reported in Liu et al. (2020). Detail explanations and assumptions regarding the choice of equations, input data, conversion of gas injection rate to hydrates deposition rate, the effects of subcooling temperatures and gas velocity on the formation of hydrates and the resulting shear stress have been discussed in the literature (Umuteme et al., 2022).

Three parameters have been investigated, including molecular viscosity of the multiphase ($\sum_q^n \alpha_q \mu_q$) and strain rate $\left(\frac{G_k}{\mu_{tq}}\right)^{1/2}$ as defined in the literature (Fluent Theory, 2017), and the shear stress, which is defined for this study as the product of the molecular viscosity of the multiphase flow and the strain rate of the secondary phase. Molecular viscosity is the resistance of the multiphase flow to shear deformation during hydrates formation. The strain rate of the water phase on the pipewall is dependent on the molecular viscosity of the flowing multiphase-induced shear stress. These parameters are measured in this study because: (i) the resisting shear strength of the hydrate layer depends on the molecular viscosity of the multiphase flow and the strain rate on the secondary water phase; (ii) the shear stress on the pipewall by the primary gas phase on the hydrates layer is directly associated with the transient pressure drop along the hydraulic profile created by the depositing hydrates; and (iii) the wearing effect of the resulting multiphase flow on the protective corrosion film on the wall of the pipe increases internal corrosion rate as the shear stress increases.

2.2 Data Analysis

Temperature, molecular viscosity, and density contour maps of the primary gas phase at the end of the simulation were extracted to define the predicted profile of the deposit of hydrates on the pipewall. Based on the stable hydrate temperature profile, the *sweep length* is a new concept introduced in this study to understand the effect of velocity on the deposition of hydrates. This study suggests that the section of the pipeline downstream from the inlet, known as the sweep length, is susceptible to pipewall shedding due to the favourable temperature and pressure conditions for hydrate formation. The sweep length extends from the point along the pipeline where hydrate formation is most likely to occur to the location where stable hydrate deposits begin to form. At the flow velocity during hydrates formation, the sweep length section is prone to the effect of pipewall shedding by hydrates, starting from the point of the onset of hydrates formation along the pipeline to the point of the onset of hydrate sloughing. The strain rate of the water phase on the pipewall was studied as indication of the severity of sloughing and wall shedding in relation to changes in subcooling temperatures and gas velocity, which also affects the deposition rates of hydrates.

2.3 Input Variables, and Boundary Conditions

The simulations were conducted for the velocity range of 2–8 m/s and the subcooling range of 5-8 K less than the fluid inlet temperature of 292 K. The natural gas operating pressure is 8.8 MPa for all simulations, which refers to the level of pressure maintained in pipeline during normal operations. It is the pressure required to ensure the safe and efficient transportation. Subsequent gas injection temperatures and pressures are determined by the mass and energy UDF codes at every time step. Heat transfer from the surrounding across the pipe to the fluid domain is by conduction, while between the liquid water and gas is by convection. The outlet pressure is predicted from the simulation at the outlet of the fluid domain. The rate of pressure drop is defined by the formation, agglomeration, and deposition of hydrates. Mass and energy source for the continuity and the momentum equations were provided by UDF codes, as discussed earlier. The simulation at higher velocity of 8 m/s and subcooling temperature of 8

K is premised on the empirical evidence that increased hydrates deposition or sloughing are mostly connected with higher subcooling temperature (Di Lorenzo et al., 2014b). Inlet multiphase flow is two phase gas-water flow, with constant water volume fraction of 0.06. The study is not replicating a previous experiment because studies on wall shedding are still exploratory in nature. However, the gas properties, flow velocities, temperature and pressure stated above are derived from experiments in the literature (Aman et al., 2016; Di Lorenzo et al., 2014a), The properties for the water phase from Ansys Fluent software have been retained. Further details of the conditions and properties of the gas and water used for this simulation have been provided in our previous work (Umuteme et al., 2022).

The hydrate thickness layers were plotted as curves in Fig. *3* for each gas flow and hydrate forming conditions. The area under each curve (AUC, m^2) is estimated from the approximation of trapezoidal method and is useful in determining the volume of deposited hydrates.

$$AUC = \frac{1}{2}\sum_{0}^{n}(h_n + h_{n-1)})\Delta L \tag{6}$$

where h, is the thickness of the deposited layer of hydrates (m) and ΔL is the hydrates-prone pipeline section. The volume of the deposited hydrates V_H (m^3), can be estimated as follows.

$$V_H = \frac{2}{3}AUC.\pi D \tag{7}$$

In Eq. (7), D is the pipe diameter (m) and π is a dimensionless constant (3.142). For the range of velocities considered in Fig. 3, the volumes of hydrates deposited are presented in Table 1, with increasing reduction in hydraulic diameter as the velocity reduces.

As reported by Turner et al. (2005) in Eq. (8), the rate of gas consumption (in kg/s) corresponds to the rate of hydrate formation. The authors established this correlation under the assumption that hydrates were exclusively formed at the condensed water-saturated gas phase. (Umuteme et al., 2022)

$$\dot{m}_{CH_4} = \frac{dm_g}{dt} = -k_1 exp\left(\frac{k_2}{T_{sys}}\right).A_i\Delta T_{sub} \tag{8}$$

In Eq. (8), the gas consumption rate ($\frac{dm_g}{dt}$; kg/s); is represented by $\dot{m}_{CH_4}$, while k_1 and k_2 are constants and A_i (m^2) denotes the interfacial area, which represents the surface area of water droplets in the gas phase. For methane hydrates, the values obtained from the experimental measurements of Vysniauskas and Bishnoi (1983) are regressed as follows: $k_1 = 7.3548 \times 10^{17}$ and $k_2 = -13600$ K. According to Turner et al. (2005), "ΔT_{sub}" the sub-cooling temperature is thermal driving force for hydrate formation, defined in Eq. (9):

$$\Delta T_{sub} = T_{eq} - T_{sys} \tag{9}$$

In Eq. (9), the hydrate deposition rate $\dot{m}_H\left(\frac{\mathrm{m}^3}{\mathrm{s}}\right)$, expressed in m^3/s, is determined as suggested in Umuteme et al. (2022) by dividing the simulated gas mass flow rate, $\dot{m}_{CH_4}$

(kg/s), by the hydrate density of 807.77 kg/m³ suggested in the literature (Balakin et al., 2016). In this context, T_{eq} represents the hydrate formation equilibrium temperature, while T_{sys} refers to the system temperature

$$\dot{m}_H\left(\frac{\mathrm{m}^3}{\mathrm{s}}\right) = \frac{\dot{m}_{CH_4}\left(\frac{\mathrm{kg}}{\mathrm{s}}\right)}{807.77\left(\frac{kg}{m^3}\right)} \tag{10}$$

3. Results and Discussion-

3.1 *Variation of Hydrates Thickness with Velocity and Subcooling Temperature*

The thickness of stable hydrate deposits on the pipewall is reconstructed from the temperature profile of the gas phase at stable hydrates forming temperature of 284K. In the discussions that follows, this understanding is extended to infer the thickness of hydrate deposits. Thus, Fig. 3 suggests that as the gas velocity increases, the thickness of the hydrates deposits decreases after a simulation duration of 4.0 s.

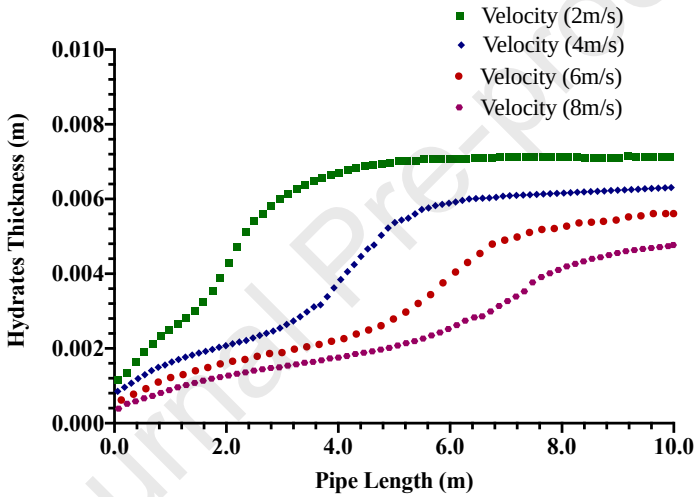

Fig. 3. Hydrates temperature profile at a subcooling temperature of 8.0 K and varying gas flow velocity of 2-8 m/s

Also, Fig. 3 indicates that the thickness of hydrates increases along the length of the pipeline from the inlet to the outlet. At a constant subcooling temperature of 8.0 K, the thickness (t) of hydrates increases as the velocity decreases. Whereas higher velocities lead to higher hydrates depositions rates (Aman et al., 2016), most of the deposited hydrates are carried along with the flow until they can be deposited at the riser base. At lower gas velocity (e.g., 2.0m/s), the risk of hydrates plugging the horizontal section of the pipeline is higher. The erosional velocity for gas lines is inversely proportional to the square root of the gas density. For gas lines the range of erosional velocity is 10-13 m/s (Mohitpour et al., 2007), however, this position did not consider the presence of hydrates in the gas stream. During the formation of hydrates, the density of gas increases towards the wall of the pipe (Umuteme et al., 2022), implying a reduction in erosional velocity from the range stated above. The literature (Zhang et al., 2020), reports that higher wall erosion rates were recorded at lower volume of deposited hydrates. Thus, from Table 1 higher pipewall erosion rates are possible at higher velocities of 8m/s., which also corroborates the empirical position in Zhang et al. (2020). As a limitation, this is an exploratory study, and we are unable to provide specific erosional velocities during pipewall shedding by hydrates at this time because this requires further experimental observation of the directional impact of hydrates on pipewall.

Table 1
Volumes of deposited hydrates at a subcooling temperature of 8.0 K and varying gas flow velocity of 2-8 m/s from Eq. (6) and (7)

Gas Velocity, V_g (m/s)	Thickness of Hydrates Deposits (mm)	Area Under Curve, AUC (m^2)	Volume of Hydrates, V_H (m^3)	Reduction in Hydraulic Diameter
2	7.13	0.0585	0.0025	69%
4	6.31	0.0430	0.0018	62%
6	5.61	0.0324	0.0014	55%
8	4.77	0.0245	0.0010	47%

The plot of the deposited hydrate volumes and the respective gas velocities indicates that the deposited volume decreases as the gas flow velocity increases.

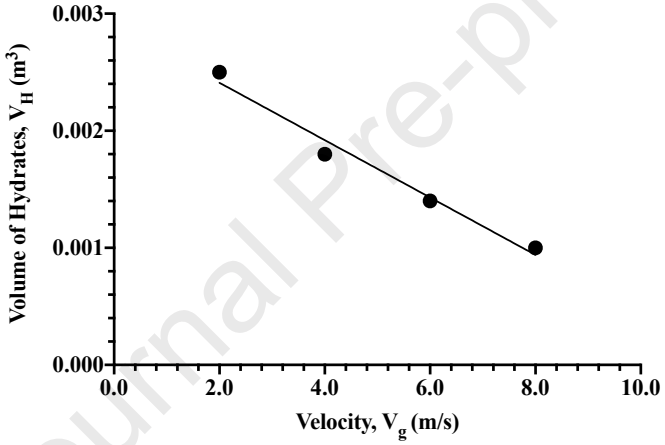

Fig. 4. The effect of increasing gas velocity on volume of deposited hydrates at subcooling temperature of 8.0 K

The volume of hydrates along the pipe reduces with increasing velocity because of increased loading of hydrates in the primary gas phase at higher gas velocities. This is a concern for the erosion of pipewall from possible increase in abrasive wear-off of the corrosion protective film on the wall. Implying that the need to transport dispersed hydrate at higher velocities must be weighed with the effect on pipewall erosion. Empirical results suggests that the depositional distance of hydrates increases with increased Reynolds number (Jassim et al., 2010). From here, the effect of hydrates sloughing and pipewall shedding is seen as primarily related to the change in gas velocity. The force to transport hydrates out of the pipeline is directly related to the resisting shear stress between the hydrates and the pipewall. However, it is still not clear if the transportability of hydrates is driven by pressure force or inertia force. The discussion that follows investigates the relationship between the fluid properties and flow dynamics during hydrates deposition, sloughing and shedding further. The shear stress experienced by the deposited hydrate layer is dependent on the molecular viscosity of the multiphase flow and the strain rate of the deposited layer of hydrates. Also, the pipewall skin friction influences the pressure drop and wall shedding by hydrates.

For a fully turbulent flow, steady state flow stabilization for a pipe of diameter (D) with an entrance length of 30D as discussed in the literature (Munson et al., 2013), hence the entry length is computed as 0.612 m. Beyond this position along the 10 m pipe section model, we

observed the temperature profile across different gas velocities and subcooling temperatures. The mass flowrate of the gas in the fluid domain provides an approximate measure of the gas consumption rate during hydrates formation, agglomeration, and deposition. The profile of hydrates in the section of the pipeline susceptible to hydrates formation is related to the concept of annular flow pattern. To provide a substantive hydrates profile, the pattern of the contour maps for the temperature and density of the gas phase were investigated. The temperature contours in Fig. **5** and Fig. 6 show the simulation results after a duration of 4.0 seconds. The gas density of the hydrate profile in Fig. **7** after a duration of 4.0 seconds was generated at 4.0 m/s gas velocity and subcooling temperature of 8.0K to demonstrate the effect of annular flow pattern in hydrates forming condition and deposition on the wall of gas pipelines.

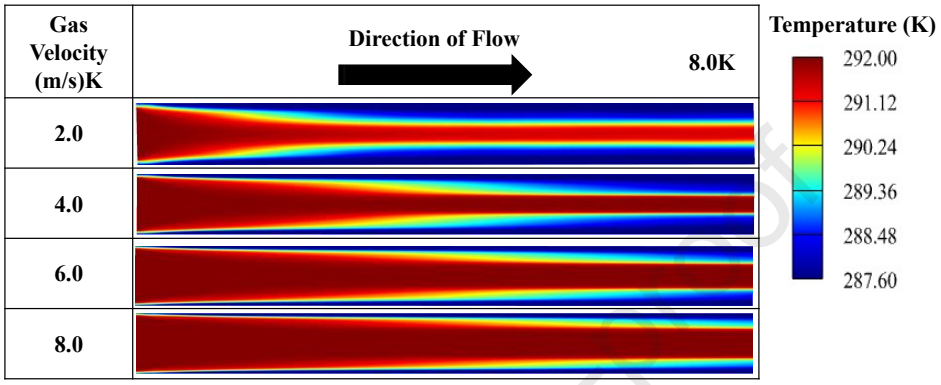

Fig. 5. Temperature profile of the gas phase at constant subcooling temperature of 8 K and varying gas velocity after a duration of 4.0 seconds. Deposited hydrates are stable below 290 K. Unstable hydrates are formed at 292 K at the core of the pipe.

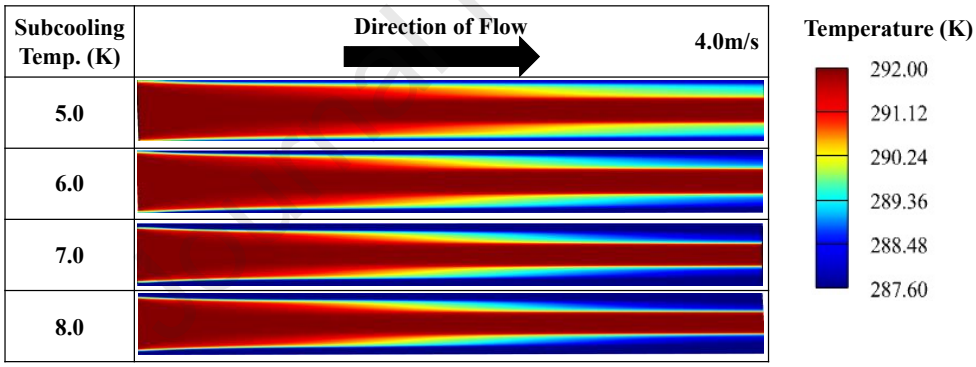

Fig. 6. Temperature profile at constant gas velocity of 4.0 m/s and varying subcooling temperature after a duration of 4.0 seconds. Deposited hydrates are stable below 290 K. Unstable hydrates are formed at 292 K at the core of the pipe.

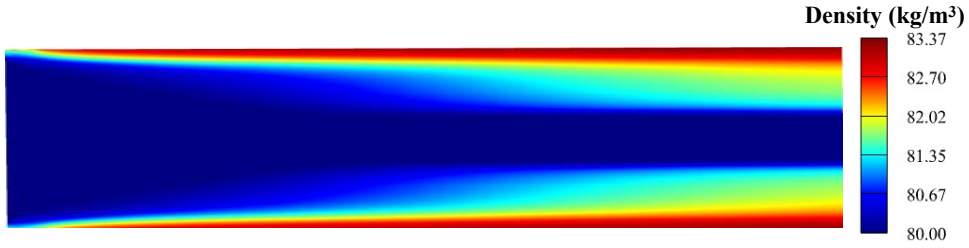

Fig. 7. Gas density profile at constant gas velocity of 4.0 m/s and subcooling temperature of 8.0 K after a duration of 4.0 seconds. The higher gas density at the wall was used to mimic hydrates deposition.

The increase of gas density towards the pipewall is supported from the literature that the volume of gas is concentrated in hydrates (Sloan, 2011). Gas density is dependent on pressure and

temperature; and increases towards the pipewall because of its lower temperature than the core. The density profile of the dense gas in **Fig. 8** can offer insights into the distribution of dense phase CO_2 in a pipeline. This can explain why there was a significant and rapid density evolution during the initial stages of dense CO_2 release from a large-scale pipeline as reported in the literature (Cao et al., 2020). As indicated earlier in Fig. 5 at lower gas velocity, there is a higher tendency of early formation of hydrate plugs in the pipeline. Also, at higher subcooling temperature and constant gas velocity, the layers of deposited hydrates create a narrow annulus at the outlet of the pipe (Fig. 6). The profile of the deposited hydrates was generated by limiting the contour map to a maximum temperature to 290 K as indicated in Fig. 9.

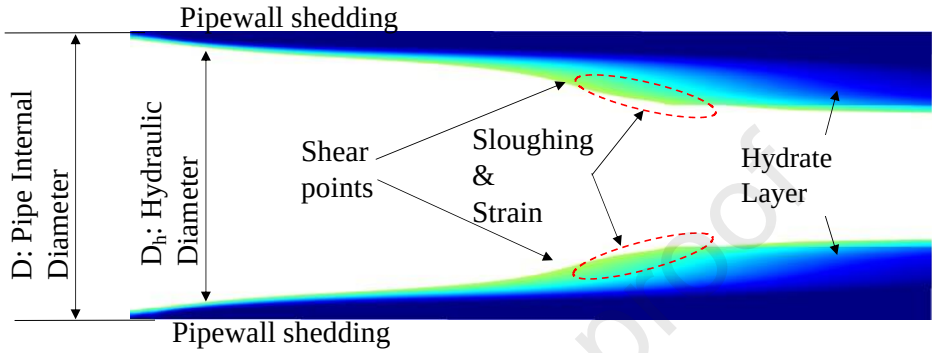

Fig. 9. Labelled profile of deposited hydrates at constant gas velocity of 4.0 m/s and subcooling temperature of 8.0 K

The profile in Fig. 9 agrees with the one proposed and discussed elsewhere (e.g., Di Lorenzo et al., 2018). Also, the location of sloughing is identified based on the hydrate profile suggested in the literature (Di Lorenzo et al., 2014b). Pipewall shedding hydrates is inferred from the thinning of the hydrate thickness represented by the dark blue layer along the pipe section. Also, the sloughing events location is inferred from the yellowish-blue layers of hydrates along the hydrates forming pipe section. It is possible to establish a relationship between the sloughing points and the velocity of the gas or the subcooling temperature from the reduction in pipe hydraulic diameter. Increase in hydrates deposition increases the shear stress at the sloughing site (Charlton et al., 2018b). In offshore gas pipelines, sloughing is responsible for delayed plugging at higher flow velocity, until the hydrates can plug the base of the riser. In our previous paper (Umuteme et al., 2022), we suggested that the shear stress varies along the pipe length at higher gas velocity instead of having a fixed value as reported by Di Lorenzo et al. (2018). A rise in transient pressure was observed as the thickness of the dark-blue hydrate layer grows into the core of the pipe section. This observation is similar to the hydrates pipe plugging effect observed in the literature (Aman et al., 2016; Di Lorenzo et al., 2014a; Liu et al., 2020).

3.2 *Effect of Velocity on the Molecular Viscosity of the Multiphase Flow*

Previous studies suggest that the formation and deposition rates of hydrates increases with increasing velocity at constant subcooling temperature (Aman et al., 2016; Di Lorenzo et al., 2014a, 2014b; Umuteme et al., 2022). Fig. 10 provides a profile of the molecular viscosity of the multiphase flow during the simulation along the pipe model. The flow is driven initially by 94% of gas volume fraction, which reduces as hydrates are formed and deposited (Umuteme et al., 2022). The increasing formation and agglomeration of hydrates increases the molecular viscosity. Thus, the fluctuating profile of the molecular viscosity of the multiphase flow during the simulation in Fig. 10 indicates the presence of turbulence, deposition and sloughing of hydrates. Pipewall shedding by hydrates also occurs intermittently. The presence of these hydraulic occurrences along the hydrates forming section of the pipe is due to increasing loading of hydrates into the continuous gas phase as the velocity increases. The initial gas viscosity at inlet condition was 0.000015 Pa-s, and the increasing viscosities in Fig. 10 is due to phase change under the hydrates forming condition of temperature, pressure, and gas

velocity. The increasing viscosity as the gas velocity increases is evidence of dispersed hydrates in the flow due to sloughing and wall shedding. The dip at the 4 m location from the inlet is the onset of sloughing. However, this sloughing is more pronounced at lower gas velocity of 2 m/s. The molecular viscosity in the entire pipeline section is relatively uniform at higher gas velocities of 6 m/s and 8 m/s. As indicated, sloughing occurred more rapidly as the flow velocity increases. The sharp drop in the value of the molecular viscosity at the 4 m location from the inlet is because of hydrates deposition and early indication of the onset of pipe plugging by hydrates. Thus, it is possible to identify the location of hydrates sloughing events along the pipeline as a critical indication of hydrates plugging risk. At the 4.6 m location, the molecular viscosity increases abruptly due to sloughing and loading of hydrates in the primary gas phase. The resisting layers of hydrate deposits can be observed at the onset of hydrates deposition at location 4 m and from location 8-10 m downstream of the inlet. Implying from Fig. 10, that the length of the resisting deposits of hydrates are as follows: 2 m at 2 m/s, 1.8 m at 4 m/s, 1.6 m at 6 m/s and 1.2 m at 8 m/s. Consequently, the length of resisting deposits of hydrates reduces as the flow velocity increases.

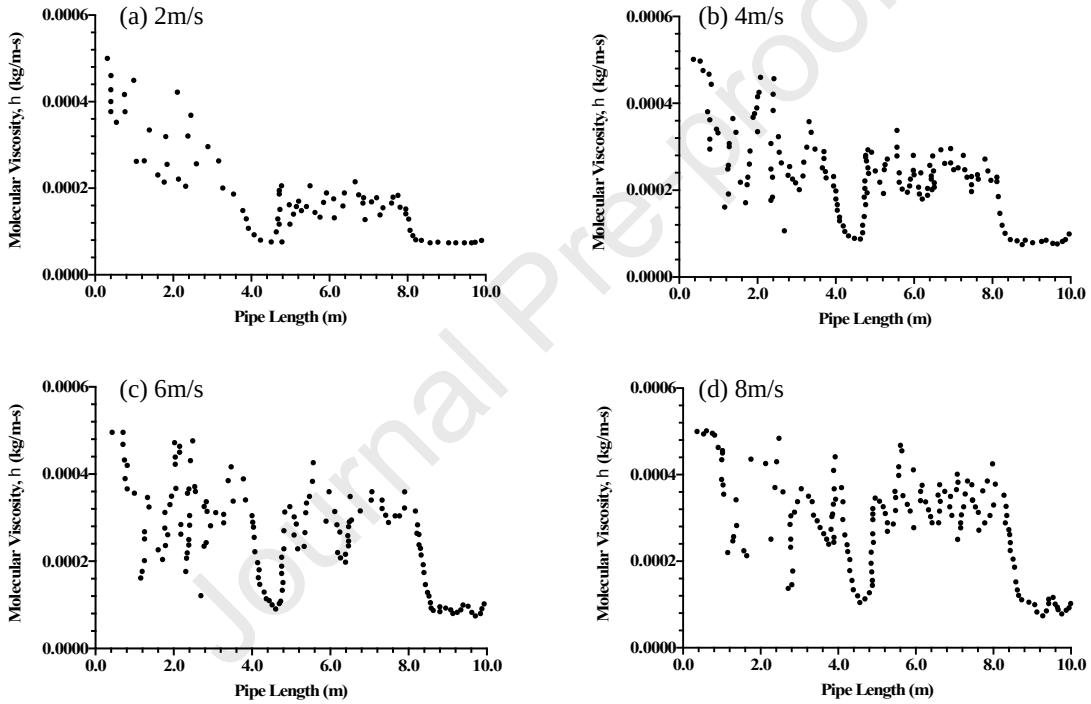

Fig. 10. Mean molecular viscosity of the multiphase flow along the horizontal cross-section of the pipe as hydrates are formed, deposited, and transported at various gas velocities and subcooling temperature of 8.0 K.

3.3 *Effect of Pipewall Friction*

Skin friction affects flow by increasing the hydraulic pressure drop along the pipeline. Also, viscous effects create a restraining force that tend to balance the pressure force (Munson et al., 2013). As discussed in Umuteme et al (2022), the turbulent Reynolds number throughout the simulation was within the transition zone where there is intermittent switch between laminar and turbulent flow. While deposition is enhanced in laminar regime, sloughing increases the turbulence in the multiphase flow, albeit at lower gas volume since gas has been consumed to form hydrates. The increasing viscosity of the flow after sloughing can lead to higher spike in system transient pressure profile. Consequently, the resistance along the flow path induces shear stress on the pipewall. Hence, the successive pressure spikes during sloughing were higher in the experiments, and it is advisable to shut down the pipeline at the onset of the first significant pressure spike during operation. The phenomenon of pipewall friction is related to the shear stress at pipewall through the Darcy friction factor f, provided in Eq. (11).

$$f = \frac{8\tau_w}{\rho V^2} \tag{11}$$

where ρ is density (kg/m^3), V is velocity (m/s) and τ_w is the wall shear stress. Fig.11 provides the pipewall skin friction factor during the simulation at the subcooling temperature of 8.0 K. The average coefficient of friction C_f values reduce as the gas velocity increases, providing evidence of the erosion of the pipewall at higher velocities.

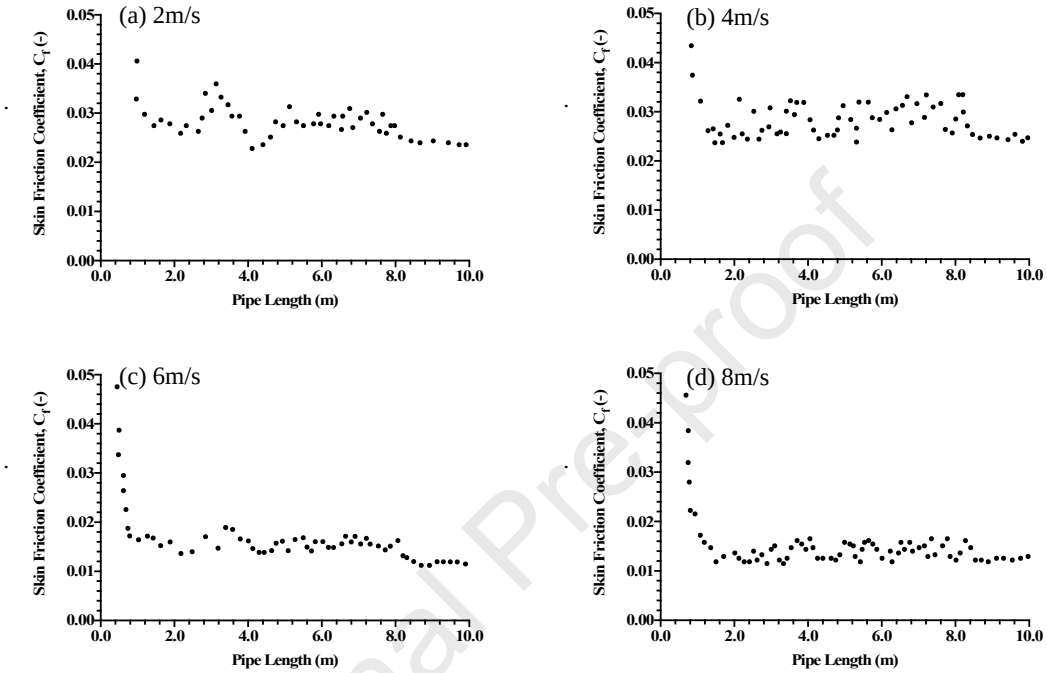

Fig.11. Increasing coefficient of pipe wall skin friction during hydrates formation, agglomeration, and deposition. The wall skin friction is obtained from the secondary water phase at subcooling temperature of 8.0 K.

3.4 *Effect of Velocity on the Strain Rate of Hydrate Deposits*

The CFD simulation results mimicked the actual effect of velocity change on the strain rate of hydrate deposits on the wall of the pipe by obtaining the strain rate data of the secondary phase in the presence of the heavier gas. Earlier in Fig. 7, it was shown that the density of the gas increased towards the pipewall because of a sustained cooling effect from the annular profile of the secondary phase. The effect of velocity on the deformation of the viscous phase by the heavier gas phase can provide insight on the carrying capacity of the gas phase and the ability to transport hydrates out of the pipe as they are formed. It is important to understand the effect of velocity on the strain rate of hydrates because hydrates shedding can damage the passive wall film on the pipe, leading to the initiation of internal corrosion (Obanijesu et al., 2011). Higher strain rate indicates higher wall shedding by hydrate deposits and a reduction of the contraction rate of the pipeline diameter. In Fig. 12, the strain rates of the deposited hydrates are compared for velocities of 2, 4, 6 and 8 m/s. In all the graphs, two zones are clearly indicated – the zone where wall shedding occurs (from inlet to the 4 m location), and the zone where sloughing occurs (4 m to 10 m). The strain rate drops at about 4 m downstream of the inlet and rises again until 2 m to the pipe exit at 2 m/s. The resistance to deformation of the hydrates deposits can be seen as positions of drops in strain rate where minimal pipewall shedding (0-4 m) and hydrates sloughing (4-10 m) occurred. The strain rate increases with increasing velocity, hence the plugging risk of hydrates is higher along the horizontal section of the pipeline at lower velocities.

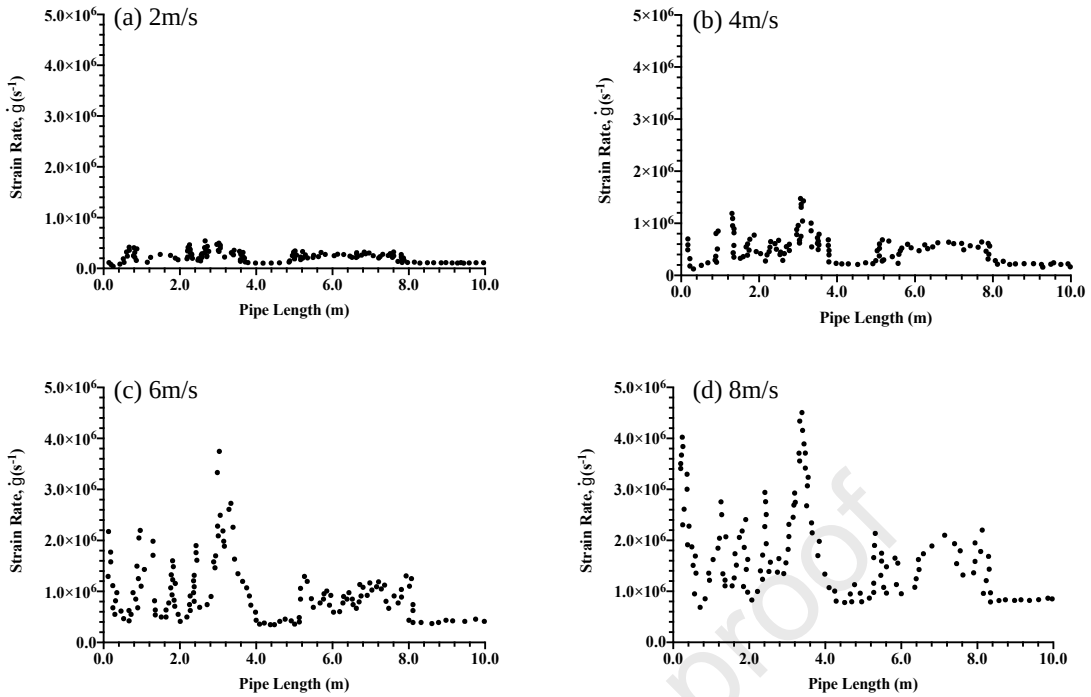

Fig. 12. The strain rate of hydrate deposits on the pipe wall

4. Hydrates Sloughing and Pipewall Shedding-

Pipewall internal corrosion resulting from the erosion of the pipewall by hydrates has been reported in the literature (Nyborg and Dugstad, 2003; Obanijesu, 2012). Thus, by simulating the conditions for hydrates formation and deposition, the profile of the deposited hydrates was captured and compared with the resulting shear stress profile. In the CFD simulations, hydrates sloughing and pipewall shedding by hydrates can be studied from the profiles of the molecular viscosity, strain rate, and shear stress. As the gas density increased towards the wall of the pipe (Fig. 7), and the molecular viscosity increases (Fig. 10), the interaction of the heavier gas phase at the wall with the water film under hydrates-condition was used to mimic the hydraulic behaviour of hydrate deposits. The simulation effect on multiphase flow pattern during hydrates formation was shown as annular from the temperature profile in Fig. 5 and Fig. 6. The locations of hydrates sloughing and pipewall shedding identified earlier in Fig. 9 are presented in Fig. 13 below. We simulated the conditions that hydrates sloughing and pipewall shedding by hydrates can happen, and we have suggested the locations based on the assumptions stated earlier and the schematics provided in the literature (Di Lorenzo et al., 2018).

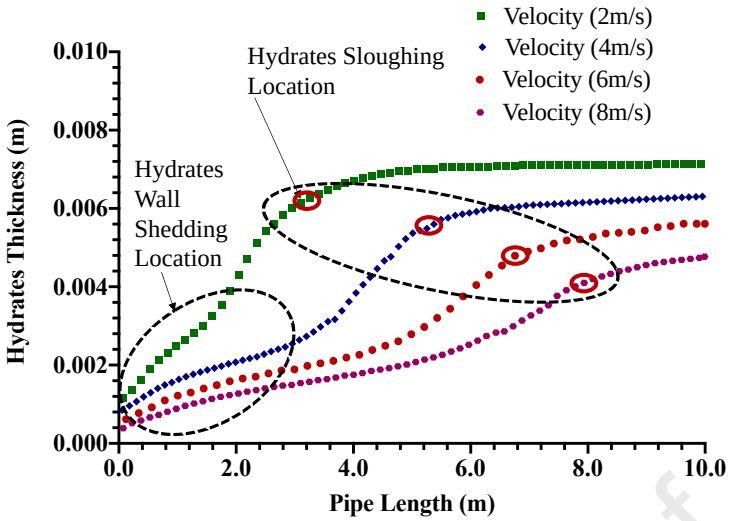

Fig. 13. Locations of hydrates sloughing and wall shedding along the pipe at the subcooling temperature of 8.0 K.

Increase in Reynolds number increases the distance of hydrates deposition along the pipe (Jassim et al., 2010). This is also evident as the profile for the gas velocity of 8 m/s indicates a father depositional distance compared to the sloughing location at the gas velocity of 2 m/s.

4.1 Sloughing and Pipewall Shedding Shear Stress

As proposed in this study, pipewall shedding by hydrates occur at the proximity of the pipe wall, with higher wall shear stress than the sloughing zone which offer higher resistance to flow. A closer synonym to shedding as implied in this study is "skinning." Thus, the discussion hereafter is how pipewall "skinning" is influenced by the shear stress of the deposited hydrates. The location of hydrates sloughing has been identified from the suggestion by Di Lorenzo et al. (2018). The shear stress plots in this section were obtained from the product of the molecular viscosity (Fig. **10**) and shear strain (Fig. **12**). The shear stress along the pipe section labelled as presented in Fig. **14**, has been compared with the respective hydrates' temperature contour at a subcooling temperature of 8.0 K and gas velocity of 4 m/s.

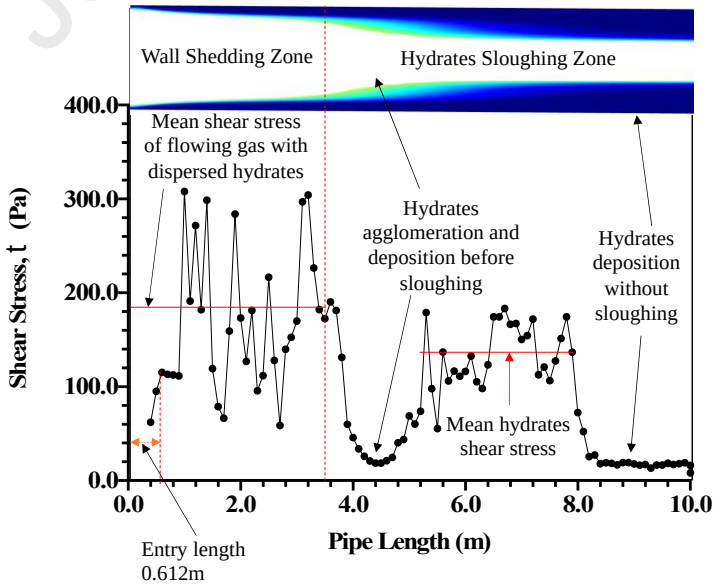

Fig. 14. Proposed representation of pipewall shedding and sloughing along the shear stress profile at 4 m/s and subcooling temperature of 8.0 K.

The plots that follow indicates the variation of shear stress with gas velocity. The reduction in wall shear stress at lower gas velocity is due to a decrease in the gradient of gas velocity at the surface of a thin film of water on the pipewall (Kundu et al., 2016). This also results in the thickening of the boundary layer. The thickening and growth of the boundary layer is analogous to the increase in hydrate deposits, which is noticed at lower velocities. The shearing stress acts on a plane perpendicular to the radial direction (Munson et al., 2013), hence able to enhance pipewall shedding as the flow velocity increases. Higher stresses are as a result of higher volume fractions of hydrates in the multiphase flow, which is also corroborated elsewhere (Jujuly et al., 2020). Also, sloughing shear stress increases with increasing gas velocity. The average pipewall shedding shear stress was obtained from between the distance of 1 m to 3 m along the pipe and increased in the following order: 2 m/s (71 Pa), 4 m/s (167 Pa), 6 m/s (259 Pa) and 8 m/s (527 Pa). The resisting sloughing average shear stress was measured from the distance of 5 m to 7 m along the pipe and increased in the order: 2 m/s (43 Pa), 4 m/s (122 Pa), 6 m/s (245 Pa) and 8 m/s (487 Pa). The maximum pipewall shedding shear strength by the hydrate layer on the pipewall recorded are above 100 Pa, in agreement with experimental predictions in Aman et al. (2018).

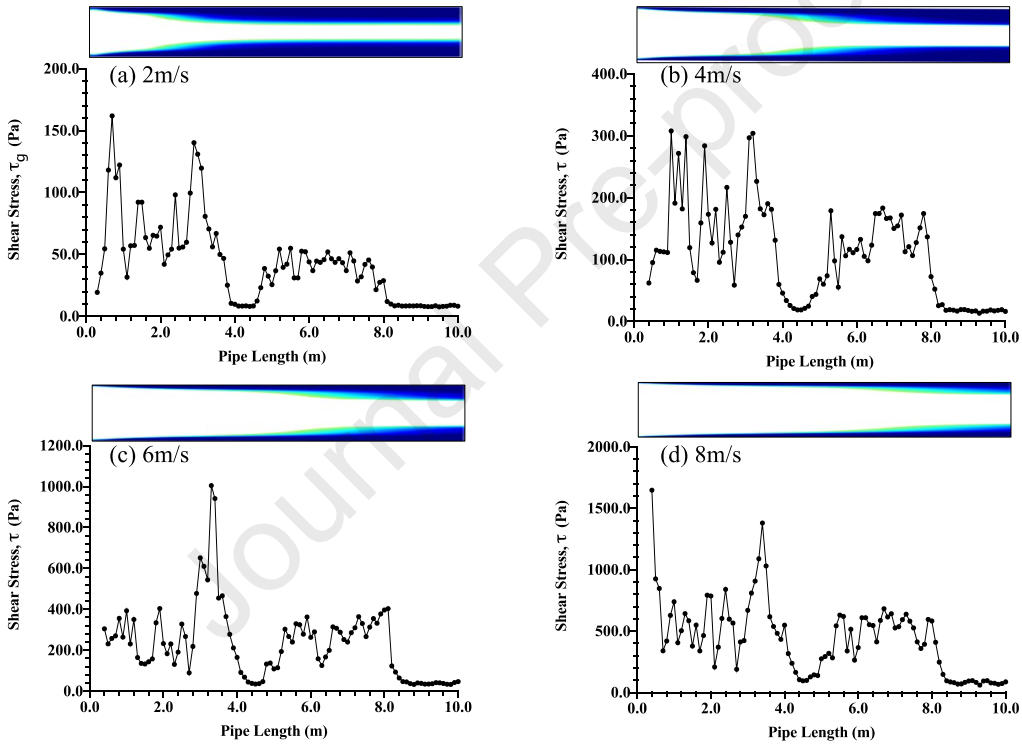

Fig. 15. Variation of shear stress with gas velocity at constant subcooling temperature of 8.0K

The risk of hydrates formation is more at higher gas velocities (Aman et al., 2016; Di Lorenzo et al., 2018; Umuteme et al., 2022), thus increasing hydrates loading and cohesiveness, with a consequential increase in flowing shear stress. The location of sloughing in a previous study was approximately 0.4575 L from the inlet of the pipeline (Liu et al., 2019). This corresponds to the 4.6 m location along the pipe length in Fig. 14 and Fig. 15. By identifying the location of hydrates sloughing corresponding to the dip at 4.0-4.6 m along the pipe length above, the pipewall shedding stress is identified as occurring before this point in this study. Although this delineation is also observable at the velocity of 6 m/s and 8 m/s in this study, the relatively uniform average shear stress profiles indicate the presence of erosion of the pipewall at higher flow velocities. Hence, while it is advisable to increase gas velocities to enhance hydrates transportability, the increasing pipewall shear stress can lead to the erosion of the pipewall. The minimum shear stress for pipewall shedding in gas-dominated pipelines is at least 100 Pa (Aman et al., 2018), and equally estimated elsewhere as 150-155 Pa (Di Lorenzo et al., 2018).

Hence, with the CFD predictions above a more effective pipewall shedding is possible at higher flow velocities. This raises a concern for low flow conditions from aging gas producing fields. From Fig. 15, the ratio of pipewall shedding shear stress to sloughing shear stress is in the order: 1.7 (2 m/s); 1.4 (4 m/s); 1.1 (6 m/s); and 8 1.1 (8 m/s). Thus, pipewall shedding and sloughing occur differently at lower gas velocities, and as the velocity increases, the distinction between pipewall shedding and sloughing reduces. Implying that higher pipewall shedding by hydrates occurs at higher gas velocities. Earlier, the wall shedding stress was obtained from the water phase on the wall of the pipe, hence the higher value of 2500 Pa at a gas velocity of 8.8 m/s. Here, the pipewall shedding stress values are obtained by multiplying the shear strain of the water phase with the molecular viscosity of the gas-water multiphase. We suggest that this approach should produce a more realistic outcome. However, this would have to be validated with field or experimental results in future.

4.2 Pressure Drop and Pipewall Shedding Shear Stress

The relationship between pipewall shear stress and pressure drop is given in the literature (Munson et al., 2013) as in Eq. (12).

$$\tau_w = \frac{D\Delta p}{4L} \tag{12}$$

where D is the CFD model pipe diameter (m), L is the model pipe length (m), τ_w is the estimated wall shear stress (Pa) and Δp is the pressure drop (Pa). However, this relation will not hold for pipe sections experiencing the deposition of hydrates because of the continual reduction in hydraulic diameter. In Eq. (12), the pressure drop reduces from the pipe inlet towards the outlet. During hydrates formation, the pressure drop is transient and peaks during agglomeration, hence Eq. (12) is unable to provide the relationship between pressure drop and pipewall shear stress in a hydrate forming gas pipeline. Transient variation in the available length of the pipeline, the hydraulic diameter and transient pressure drop will be discussed further. The available length is the hydrates forming section of the pipeline less the hydrates plugging section and have been identified as the sweep length in this study. In Fig.**16** the sweep length (L_{sw}) is the section of the pipe where pipewall shedding is prevalent.

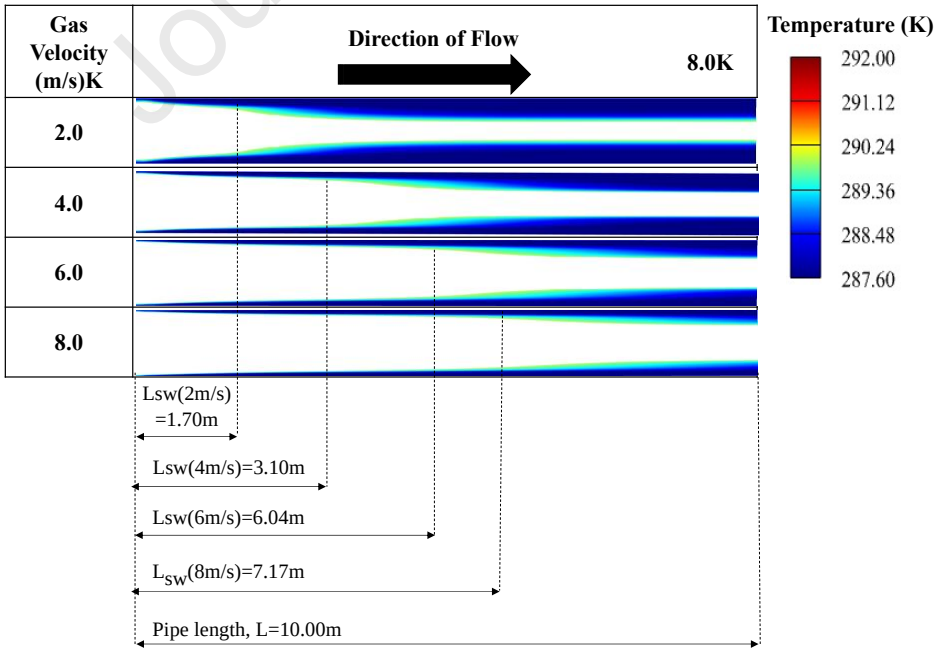

Fig.16. Variation of hydrates sweep length with varying gas velocity at constant subcooling temperature of 8.0 K. The sweep length represents the hydrates wall shedding section along the pipe.

The sweep length terminates at the onset of hydrates sloughing. The sweep length increases with increasing velocity, suggesting that higher gas velocities can enhance hydrates transportability, but can also lead to higher pipewall shedding. The hydraulic diameter for the sweep length section (D_{h_sw}), is expected to be uniform since the pipewall is "skinned," so to say. Another term, the sweep ratio (S_{sw_r}), was introduced to relate the sweep length, L_{sw} to the length of the hydrates forming section of the pipeline, L. As seen in Fig.17, the S_{sw_r} increases with increasing gas velocity.

$$S_{sw\_r} = \frac{L_{sw}}{L} \tag{13}$$

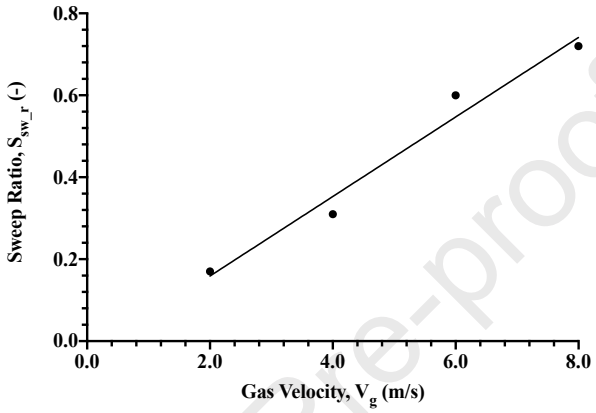

Fig.17. Effect of gas velocity on sweep ratio at a subcooling temperature of 8.0K.

The ratio of transient pressure drop is compared with the inertia force using the dimensionless Euler number ratio (Eu) in Eq. (14). In Fig.18, $Eu < 1$ for all gas velocities, showing that pipewall shedding and sloughing are driven by inertia force rather than the transient pressure. A more resisting flow is observed at 2 m/s, again suggesting higher plugging risk at lower gas velocities.

$$Eu = \frac{\Delta p}{\rho {V_g}^2} \tag{14}$$

where Δp, ρ, and V_g retains their earlier definitions.

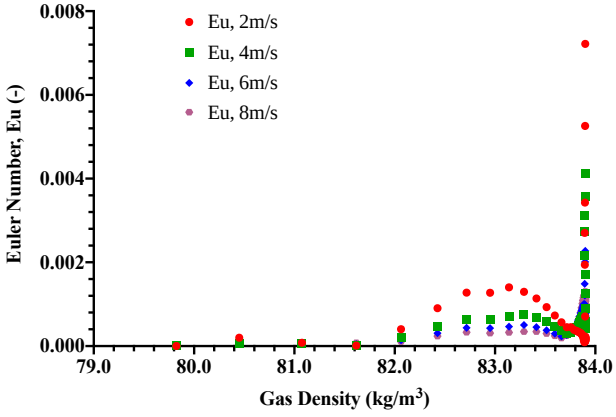

Fig.18. Effect of change in the density of the gas on the Euler number at a subcooling temperature of 8.0 K.

A further analysis of Fig. **13** by defining the 'sloughing angle (θ_{sl})' as a new term unique to this paper, suggests that the sloughing angle increases with increasing velocity. This can be inferred from the deposition rates in the literature (Umuteme et al., 2022), as the gas velocity increases under the same subcooling temperature.

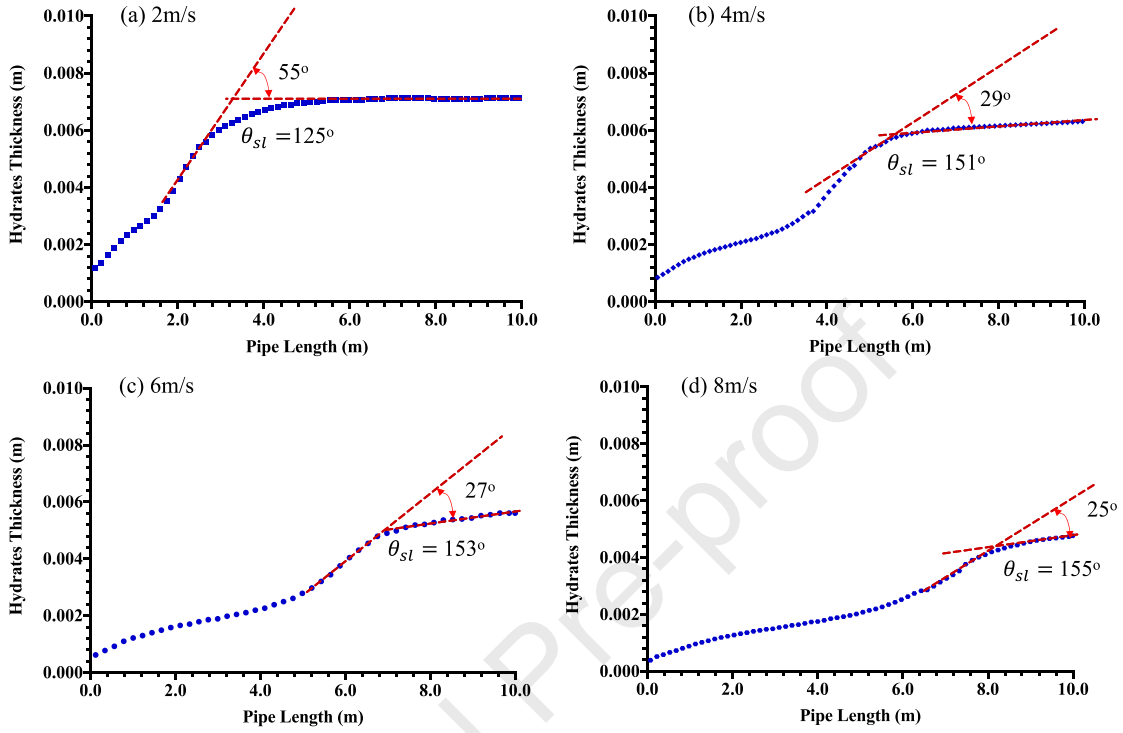

Fig.19. Hydrates profile at a subcooling temperature of 8.0K and varying gas flow velocity. (a) 2 m/s – sloughing angle of 125°. (b) 4 m/s – sloughing angle of 151°. (c) 6 m/s – sloughing angle of 153°. (d) 8 m/s – sloughing angle of 155°.

Thus, the steepness of the deposited hydrates profile increases as the gas velocity increases and can lead to delayed plugging of the pipeline at higher fluid flow velocities. A higher reduction of 69% in hydraulic diameter was earlier at the velocity of 2 m/s (Fig.20).

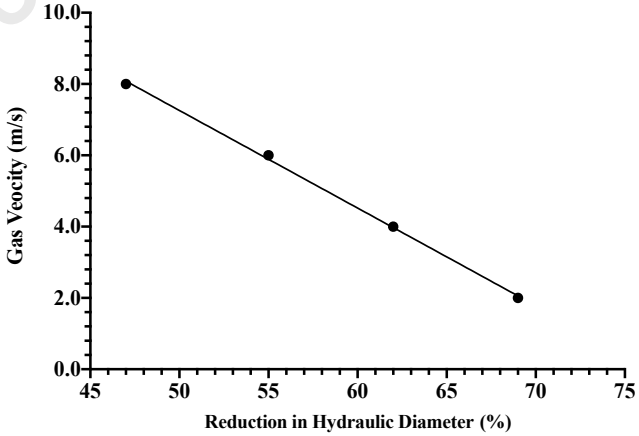

Fig.20. Effect of sloughing on pipeline hydraulic diameter at a subcooling temperature of 8.0K and varying gas flow velocity.

Finally, the effect of sloughing and pipewall shedding shear stress in a hydrate forming pipeline can be inferred from the simulation results for the velocities of the gas and dispersed water phase at 8.8 m/s and the pipewall subcooling temperature of 7.0K in Fig.21. As indicated in Fig.21, the velocity of the water phase is below that of the primary gas phase albeit both having

the same inlet velocity, suggesting an increasing resistance to flow by the water phase. The drop in the velocity of both phases is due to reduction in volume and obstruction to flow because of phase change and increase in viscosity. Implying that as the viscosity increases due to more deposition of hydrates, there will be a decrease in both sloughing and pipewall shedding events, and the pipeline will finally get plugged by hydrates.

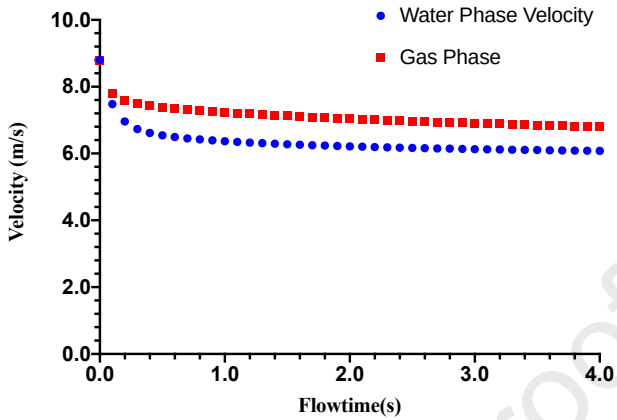

Fig.21. Velocity profile of gas and water phase during hydrates formation at a subcooling temperature of 7.0K.

5. Conclusion-

This study simulated the conditions necessary for hydrates formation and deposition in a gas pipeline using the validated CFD model that was developed in our preceding paper (Umuteme et al., 2022). The need for this study was to enrich the literature on hydrates sloughing/shedding and pipewall shedding by hydrates. Previous research confused hydrates shedding with pipewall shedding by hydrates, hence shedding was seen as hydrates "falling off" the pipewall under the influence of a viscous force. This study suggests that pipewall shedding is erosive in nature under the influence of the shear stress of the gas-water-dispersed hydrate multiphase flow, and occurs behind the sloughing zone. The geometry of hydrate deposits (Di Lorenzo et al., 2018) and the plot of the thickness of hydrate deposits along the pipeline (Liu et al., 2019), indicates that a three phase gas, water and dispersed hydrates multiphase flow upstream of the hydrates sloughing point exists. Hence, it is important to emphasis the effect of a dispersed hydrates phase on the pipewall. The shear stress profile along the pipeline provide insight on the effect of pipewall shedding by hydrates. The CFD simulation adopted in this study mimicked hydrates deposition by applying a subcooling temperature to the pipe wall at hydrates formation condition to increase the density of the gas at the wall and enhance the viscous interaction of the gas phase with the water phase at the annular water layer at the wall. The simulated temperature contour profile captured the expected cooling effect on the gas phase similar to the hydrates deposit geometry in the literature (Di Lorenzo et al., 2018). The plots of molecular viscosity of the multiphase and strain rate of the secondary phase indicated a dip which agrees with the relative location of sloughing events in the literature from the inlet of the pipeline (Liu et al., 2019). Finally, this study proposes that:

a) Hydrates sloughing is predominant at lower gas velocities, happening over a longer distance along the hydrates forming section until the pipeline is plugged.
b) Higher reduction in hydraulic diameter is earlier at lower gas velocities
c) The profile of the deposited hydrates is steeper at higher velocities as indicated by the sloughing angle, which is a new term developed in this study. The lower the sloughing angle the longer the sloughing event along the pipeline and can lead to a gentle profiling of hydrates layer over a longer section of the pipeline. Thus, hydrates plugs are longer at lower velocities than at higher velocities. Implying a higher plugging risk at lower velocities.

d) At lower gas velocities pipewall shedding leads to higher shear stress values when compared with the shear stress at the sloughing location. This observation occurred at velocities of 2.0 m/s and 4.0 m/s.
e) Pipewall shedding and sloughing occurs simultaneously at higher gas velocities. This was observed at 6.0 m/s and 8.0 m/s.
f) The fluctuating plots of shear stress suggests that hydrates sloughing events and pipewall shedding by hydrates occurs intermittently and can lead to flow induced vibration along the pipeline (Nicholas et al., 2008). This proposition substantiates the outcome reported in elsewhere (Jujuly et al., 2017).
g) The shear stress profile along a hydrate forming gas pipeline can enhance the determination of locations prone to higher corrosion rates.
h) Hydrates sloughing and pipewall shedding are driven by inertia force, instead of transient pressure drop.
i) This simulations in the study did not account for hydrate as a discreet phase. We have only simulated the temperature and pressure condition for hydrate formation, deposition and pipewall shedding. It is recommended that future studies should account for the effect of hydrate particles on the pipewall.

Acknowledgement
The authors are grateful to the School of Engineering, Robert Gordon University, Aberdeen, United Kingdom, for supporting this research.

Conflicts of Interest
The authors declare no conflicts of interest.

Nomenclature

A: Pipe cross-sectional area (m^2)
A_i: Interfacial area (m^2)
C_μ: Turbulent viscosity constant (-)
$C_{1\varepsilon}$ and $C_{2\varepsilon}$: Constants (-)
D: Diameter of the pipe section prone to hydrate formation (m)
D_h: Pipeline hydraulic diameter (m)
D_{h_sw}: Pipeline hydraulic diameter at the end of the sweep length (m)
$G_{k,q}$: Turbulent kinetic energy production term per phase (-)
h_q: The q^{th}phase specific enthalpy (J/kg)
h_{pq}: Interphase enthalpy (J/kg)
k_1 and k_2: Constants (-)
k: Turbulent kinetic energy rate (m^2s^{-3})
k:Turbulent kinetic energy (J/kg)
L_{sw}: The difference between the length of the pipe and the uniform section of hydrates layer (m)
$\dot{m}_{CH_4}$: Methane gas consumption rate ($\frac{dm_g}{dt}$) (Kg/s)
$\dot{m}_H$: Hydrate deposition rate (m^3/s)
v_g: Velocity of the primary continuous gas phase (m/s)
$\vec{\vartheta}_q$: Velocity vector of the phase in the control volume (m/s)
S_q: Source/sink term: gas consumption rate or source energy rate (Kg/s-m^3 or J/s-m^3)
S_{sw_r}: Ratio of the sweep length to the length of the hydrates section along the gas pipeline (-)
T_{eq}: Hydrate formation equilibrium temperature (K)
T_{sys}: System temperature (K)

Greek Symbol

α_q: Phase fraction (-)

ε: Turbulent dissipation rate (m^2s^{-3})

ρ_q: Density of the phase (kg/m^3)

ρ_q: Density of the q^{th} phase (kg/m^3)

μ_{tq}: Turbulent viscosity of the q^{th} phase ($Nm^{-2}.s$, Pa.s)

Δp: Pressure drop (Pa)

Π_{k_q} and Π_{ε_q}: Source terms for the turbulence interactions of the entrained water phase on the primary gas phase (Π_{k_q}: turbulent and Π_{ε_q}: dissipation)

θ_{sl}: Sloughing angle (-)

τ_w: Pipewall Shear Stress (Pa)

References:

Aman, Z.M., Di Lorenzo, M., Kozielski, K., Koh, C.A., Warrier, P., Johns, M.L., May, E.F., 2016. Hydrate formation and deposition in a gas-dominant flowloop: Initial studies of the effect of velocity and subcooling. J. Nat. Gas Sci. Eng. 1–9. https://doi.org/10.1016/j.jngse.2016.05.015

Aman, Z.M., Qin, H., Pickarts, M., Lorenzo, M. Di, May, E.F., Koh, C.A., Zerpa, L.E., 2018. Deposition and shear stress initial investigations for hydrate blockage, in: Proceedings of the Annual Offshore Technology Conference. https://doi.org/10.4043/28777-ms

Balakin, B. V, Lo, S., Kosinski, P., Hoffmann, A.C., 2016. Modelling agglomeration and deposition of gas hydrates in industrial pipelines with combined CFD-PBM technique. Chem. Eng. Sci. 153. https://doi.org/10.1016/j.ces.2016.07.010

Barrie, J., Brown, K., Hatcher, P.R., Schellhase, H.U., 2005. Carbon dioxide pipelines: A preliminary review of design and risks. Greenh. Gas Control Technol. 315–320. https://doi.org/10.1016/B978-008044704-9/50032-X

Bataille, C., Åhman, M., Neuhoff, K., Nilsson, L.J., Fischedick, M., Lechtenböhmer, S., Solano-Rodriquez, B., Denis-Ryan, A., Stiebert, S., Waisman, H., Sartor, O., Rahbar, S., 2018. A review of technology and policy deep decarbonization pathway options for making energy-intensive industry production consistent with the Paris Agreement. J. Clean. Prod. 187, 960–973. https://doi.org/10.1016/j.jclepro.2018.03.107

Cao, Q., Yan, X., Liu, S., Yu, J., Chen, S., Zhang, Y., 2020. Temperature and phase evolution and density distribution in cross section and sound evolution during the release of dense CO2 from a large-scale pipeline. Int. J. Greenh. Gas Control 96. https://doi.org/10.1016/j.ijggc.2020.103011

Carroll, J., 2014. Natural Gas Hydrates: A Guide for Engineers, 3rd ed. Gulf Professional Publishing, Waltham, MA 02451.

Charlton, T.B., Di Lorenzo, M., Zerpa, L.E., Koh, C.A., Johns, M.L., May, E.F., Aman, Z.M., 2018a. Simulating Hydrate Growth and Transport Behavior in Gas-Dominant Flow. Energy and Fuels 32, 1012–1023. https://doi.org/10.1021/acs.energyfuels.7b02199

Charlton, T.B., Zerpa, L.E., Koh, C.A., May, E.F., Aman, Z.M., 2018b. Predicting hydrate blockage formation in gas-dominant systems, in: Offshore Technology Conference Asia 2018, OTCA 2018. Offshore Technology Conference. https://doi.org/https://doi.org/10.4043/28311-ms

Di Lorenzo, M., Aman, Z.M., Kozielski, K., Norris, B.W.E., Johns, M.L., May, E.F., 2018. Modelling hydrate deposition and sloughing in gas-dominant pipelines. J. Chem. Thermodyn. 117, 81–90. https://doi.org/10.1016/j.jct.2017.08.038

Di Lorenzo, M., Aman, Z.M., Kozielski, K., Norris, B.W.E., Johns, M.L., May, E.F., 2014a.

Underinhibited hydrate formation and transport investigated using a single-pass gas-dominant flowloop. Energy and Fuels 28, 7274–7284. https://doi.org/10.1021/ef501609m

Di Lorenzo, M., Aman, Z.M., Sanchez Soto, G., Johns, M., Kozielski, K.A., May, E.F., 2014b. Hydrate formation in gas-dominant systems using a single-pass flowloop. Energy and Fuels 28, 3043–3052. https://doi.org/10.1021/ef500361r

Fluent Theory, 2017. ANSYS fluent theory guide version 18.1. ANSYS, Inc., 275 Technology Drive Canonsburg,., 275 Technology Drive Canonsburg, PA 15317.

Fox, R.O., 2014. On multiphase turbulence models for collisional fluid-particle flows. J. Fluid Mech. 742, 368–424. https://doi.org/10.1017/jfm.2014.21

Gough, C., O'Keefe, L., Mander, S., 2014. Public perceptions of CO2 transportation in pipelines. Energy Policy 70, 106–114. https://doi.org/10.1016/j.enpol.2014.03.039

Jassim, E., Abdi, M.A., Muzychka, Y., 2010. A new approach to investigate hydrate deposition in gas-dominated flowlines. J. Nat. Gas Sci. Eng. 2, 163–177. https://doi.org/10.1016/j.jngse.2010.05.005

Jujuly, M.M., Rahman, M.A., Maynard, A., Addy, M., 2017. Hydrate induced vibration in an offshore pipeline, in: Proceedings - SPE Annual Technical Conference and Exhibition. https://doi.org/10.2118/187378-ms

Jujuly, M.M., Rahman, M.A., Maynard, A., Adey, M., 2020. Hydrate-Induced Vibration in an Offshore Pipeline. SPE J. 25. https://doi.org/10.2118/187378-pa

Kundu, P.K., Cohen, I.M., Dowling, D.R., 2016. Fluid mechanics, 6th ed. Academic Press.

Lekvam, K., Bishnoi, P.R., 1997. Dissolution of methane in water at low temperatures and intermediate pressures. Fluid Phase Equilib. 131, 297–309. https://doi.org/10.1016/s0378-3812(96)03229-3

Liu, W., Hu, J., Wu, K., Sun, F., Sun, Z., Chu, H., Li, X., 2019. A new hydrate deposition prediction model considering hydrate shedding and decomposition in horizontal gas-dominated pipelines. Pet. Sci. Technol. 37, 1370–1386. https://doi.org/10.1080/10916466.2019.1587457

Liu, Z., Vasheghani Farahani, M., Yang, M., Li, X., Zhao, J., Song, Y., Yang, J., 2020. Hydrate slurry flow characteristics influenced by formation, agglomeration and deposition in a fully visual flow loop. Fuel 277, 118066. https://doi.org/10.1016/j.fuel.2020.118066

Lu, H., Ma, X., Huang, K., Fu, L., Azimi, M., 2020. Carbon dioxide transport via pipelines: A systematic review. J. Clean. Prod. 266. https://doi.org/10.1016/j.jclepro.2020.121994

May, E.F., Lim, V.W., Metaxas, P.J., Du, J., Stanwix, P.L., Rowland, D., Johns, M.L., Haandrikman, G., Crosby, D., Aman, Z.M., 2018. Gas Hydrate Formation Probability Distributions: The Effect of Shear and Comparisons with Nucleation Theory. Langmuir 34, 3186–3196. https://doi.org/10.1021/acs.langmuir.7b03901

Meindinyo, R.E.T., Svartaas, T.M., Nordbø, T.N., Bøe, R., 2015. Gas hydrate growth estimation based on heat transfer. Energy and Fuels 29, 587–594. https://doi.org/10.1021/ef502366u

Mohitpour, M., Golshan, H., Murray, A., 2007. Pipeline Design & Construction: A Practical Approach, Third Edition, 3rd ed. ASME Press, New York. https://doi.org/10.1115/1.802574

Munson, B.R., Okiishi, T.H., Huebsch, W.W., Rothmayer, A.P., 2013. Fundamentals of Fluid Mechanics, 7th ed. John Wiley & Sons, Inc., Hoboken, NJ.

Nicholas, J.W., Inman, R.R., Steele, J.P.H., Koh, C.A., Sloan, E.D., 2008. A modeling approach to hydrate wall growth and sloughing in a water saturated gas pipeline, in:

Proceedings of the 6th International Conference on Gas Hydrates (ICGH 2008), Vancouver, British Columbia, CANADA, July 6-10, 2008.

Nyborg, R., Dugstad, A., 2003. Understanding and Prediction of Mesa Corrosion Attack. Corros. 2003.

Obanijesu, E.O., 2012. Corrosion and Hydrate Formation in Natural Gas Pipelines 239.

Obanijesu, E.O., 2009. Modeling the H2S contribution to internal corrosion rate of natural gas pipeline. Energy Sources, Part A 31, 348–363. https://doi.org/10.1080/15567030701528408

Obanijesu, E.O., Akindeju, M.K., Vishnu, P., Tade, M.O., 2011. Modelling the Natural Gas Pipeline Internal Corrosion Rate Resulting from Hydrate Formation, Computer Aided Chemical Engineering. Elsevier B.V. https://doi.org/10.1016/B978-0-444-54298-4.50011-8

Odutola, T.O., Ajienka, J.A., Onyekonwu, M.O., Ikiensikimama, S.S., 2017. Fabrication and Validation of a Laboratory Flow Loop for Hydrate Studies. Am. J. Chem. Eng. Spec. Issue Oil F. Chem. Petrochemicals 5, 28–41. https://doi.org/10.11648/j.ajche.s.2017050301.14

Simonin, O., Viollet, P.L., 1990. Predictions of an Oxygen Droplet Pulverization in a Compressible Subsonic Coflowing Hydrogen Flow. Numer. Methods Multiph. Flows FED91 FED91, 65–82.

Sloan, D.E., Koh, C.A., 2007. Clathrate hydrates of natural gases, 3rd ed, Clathrate Hydrates of Natural Gases, Third Edition. CRC Press, Boca Raton, FL.

Sloan, E., 2011. Introduction: What are hydrates?, in: Sloan, D., Koh, C.A., Sum, A.K. (Eds.), Natural Gas Hydrates in Flow Assurance. Gulf Professional Publishing is an imprint of Elsevier. https://doi.org/10.1016/C2009-0-62311-4

Straume, E.O., Kakitani, C., Salomão, L.A.S., Morales, R.E.M., Sum, A.K., 2018. Gas Hydrate Sloughing as Observed and Quantified from Multiphase Flow Conditions. Energy & Fuels 32, 3399–3405. https://doi.org/10.1021/acs.energyfuels.8b00246

Turner, D., Boxall, J., Yang, D., Kleehamer, C., Koh, C., Miller, K., Sloan, E.D., Yang, S., Xu, Z., Mathews, P., Talley, L., 2005. Development of a Hydrate Kinetic Model and Its Incorporation Into the OLGA2000® Transient Multi-Phase Flow Simulator. Proc. 5th Int. Conf. Gas Hydrates.

Umuteme, O.M., Islam, S.Z., Hossain, M., Karnik, A., 2022. An improved computational fluid dynamics (CFD) model for predicting hydrate deposition rate and wall shear stress in offshore gas-dominated pipeline. J. Nat. Gas Sci. Eng. 107. https://doi.org/10.1016/j.jngse.2022.104800

Vysniauskas, A., Bishnoi, P.R., 1983. A kinetic study of methane hydrate formation. Chem. Eng. Sci. 38. https://doi.org/10.1016/0009-2509(83)80027-X

Wang, Z., Li, Y., Tong, X., Gong, J., 2022. Risk probability evaluation for the effect of obstacle on CO2 leakage and dispersion indoors based on uncertainty theory. J. Loss Prev. Process Ind. 74. https://doi.org/10.1016/j.jlp.2021.104652

Wang, Z., Zhang, J., Chen, L., Zhao, Y., Fu, W., Yu, J., Sun, B., 2018. Modeling of hydrate layer growth in horizontal gas-dominated pipelines with free water. J. Nat. Gas Sci. Eng. 50, 364–373. https://doi.org/10.1016/j.jngse.2017.11.023

Wang, Z., Zhang, J., Sun, B., Chen, L., Zhao, Y., Fu, W., 2017. A new hydrate deposition prediction model for gas-dominated systems with free water. Chem. Eng. Sci. 163, 145–154. https://doi.org/10.1016/j.ces.2017.01.030

Wareing, C.J., Fairweather, M., Falle, S.A.E.G., Woolley, R.M., Ward, A.M.E., 2016. High pressure CO2 CCS pipelines: Comparing dispersion models with multiple experimental

datasets. Int. J. Greenh. Gas Control 54, 716–726. https://doi.org/10.1016/j.ijggc.2016.08.030

Zerpa, L.E., Rao, I., Aman, Z.M., Danielson, T.J., Koh, C.A., Sloan, E.D., Sum, A.K., 2013. Multiphase flow modeling of gas hydrates with a simple hydrodynamic slug flow model. Chem. Eng. Sci. 99, 298–304. https://doi.org/10.1016/j.ces.2013.06.016

Zhang, L., Zhou, J.W., Zhang, B., Gong, W., 2020. Numerical investigation on the solid particle erosion in elbow with water–hydrate–solid flow. Sci. Prog. 103. https://doi.org/10.1177/0036850419897245

Table 1
Volumes of deposited hydrates at a subcooling temperature of 8.0 K and varying gas flow velocity of 2-8 m/s from Eq. **Error! Reference source not found.** and **Error! Reference source not found.**

Gas Velocity, V_g (m/s)	Thickness of Hydrates Deposits (mm)	Area Under Curve, AUC (m^2)	Volume of Hydrates, V_H (m^3)	Reduction in Hydraulic Diameter
2	7.13	0.0585	0.0025	69%
4	6.31	0.0430	0.0018	62%
6	5.61	0.0324	0.0014	55%
8	4.77	0.0245	0.0010	47%

Declaration of interests

☒ The authors declare that they have no known competing financial interests or personal relationships that could have appeared to influence the work reported in this paper.

☐The authors declare the following financial interests/personal relationships which may be considered as potential competing interests: